Johanson, R. A., & Colman, R. F. (1981a) *Arch. Biochem. Biophys. 207*, 9–20.
Johanson, R. A., & Colman, R. F. (1981b) *Arch. Biochem. Biophys. 207*, 21–31.
Kapetanovic, E., Bailey, J. M., & Colman, R. F. (1985) *Biochemistry 24*, 7586–7593.
Lanzetta, P. A., Alvarez, L. J., Reinach, P. S., & Candia, O. A. (1979) *Anal. Biochem. 100*, 95–97.
Marquardt, D. W. (1963) *J. Soc. Ind. Appl. Math. 11(2)*, 431–441.
Mas, M. T., & Colman, R. F. (1983) *J. Biol. Chem. 258*, 9332–9338.
Mas, M. T., & Colman, R. F. (1984) *Biochemistry 23*, 1675–1683.
Mas, M. T., & Colman, R. F. (1985) *Biochemistry 24*, 1634–1646.
Meyer, R. B., Shuman, D. A., Robins, R. K., Miller, J. P., & Simon, L. N. (1973) *J. Med. Chem. 16*, 1319–1323.
Penefsky, H. S. (1977) *J. Biol. Chem. 252*, 2891–2899.
Rappe, C. (1963) *Ark. Kemi 21*, 503–516.
Riordan, J. F. (1973) *Biochemistry 12*, 3915–3923.
Rippa, M., Sigornini, M., Signori, R., & Dallocchio, F. (1975) *FEBS Lett. 51*, 281–283.
Schleich, T., Cross, B. P., Blackburn, B. J., & Smith, I.C.P. (1975) *Structure and Conformation of Nucleic Acids and Protein–Nucleic Acid Interactions* (Sundaralingam, M., & Rao, S. T., Eds.) pp 223–252, University Park Press, Baltimore, MD.
Yankeelov, J. A., Jr. (1970) *Biochemistry 9*, 2433–2439.
Zall, D. M., Fisher, D., & Garner, M. Q. (1956) *Anal. Chem. 28*, 1665–1668.

# Accuracy of Alternative Representations for Integrated Biochemical Systems†

Eberhard O. Voit‡ and Michael A. Savageau*
*Department of Microbiology and Immunology, The University of Michigan, Ann Arbor, Michigan 48109*
*Received November 26, 1986; Revised Manuscript Received June 10, 1987*

ABSTRACT: The Michaelis–Menten formalism often provides appropriate representations of individual enzyme-catalyzed reactions in vitro but is not well suited for the mathematical analysis of complex biochemical networks. Mathematically tractable alternatives are the linear formalism and the power-law formalism. Within the power-law formalism there are alternative ways to represent biochemical processes, depending upon the degree to which fluxes and concentrations are aggregated. Two of the most relevant variants for dealing with biochemical pathways are treated in this paper. In one variant, aggregation leads to a rate law for each enzyme-catalyzed reaction, which is then represented by a power-law function. In the other, aggregation produces a composite rate law for either net rate of increase or net rate of decrease of each system constituent; the composite rate laws are then represented by a power-law function. The first variant is the mathematical basis for a method of biochemical analysis called metabolic control, the latter for biochemical systems theory. We compare the accuracy of the linear and of the two power-law representations for networks of biochemical reactions governed by Michaelis–Menten and Hill kinetics. Michaelis–Menten kinetics are always represented more accurately by power-law than by linear functions. Hill kinetics are in most cases best modeled by power-law functions, but in some cases linear functions are best. Aggregation into composite rate laws for net increase or net decrease of each system constituent almost always improves the accuracy of the power-law representation. The improvement in accuracy is one of several factors that contribute to the wide range of validity of this power-law representation. Other contributing factors that are discussed include the nonlinear character of the power-law formalism, homeostatic regulatory mechanisms in living systems, and simplification of rate laws by regulatory mechanisms in vivo.

Biochemical systems are often difficult to understand intuitively. Even simple feedback loops can exhibit very different types of behavior: system components may quickly return to the original or a new steady-state after perturbation, they may oscillate in a stable cycle, or the entire system may become unstable. It is evident that the repertoire of behavior for a system with many components and with activating and inhibiting interactions is much wider. The central problem in understanding the function of intact biochemical systems is the large number and the complex nonlinear character of interactions among the molecular constituents (Savageau, 1976, 1985a). This problem is in general too complex to be solved intuitively and requires systematic mathematical models and analyses.

Since the turn of the century, a variety of mathematical functions have been proposed that approximate single reactions reasonably well in vitro and presumably in vivo. The most familiar are the Michaelis–Menten rate law (Michaelis & Menten, 1913) and the Hill rate law (Brown & Hill, 1923). Both equations are simple rational functions, whose properties are readily calculated as long as only one reaction or a system of very few reactions is being studied. However, under physiological conditions, each reaction is embedded in an intricate network of reactions, subject to general buffers and specific modulations, which makes mathematical analysis with Michaelis–Menten or Hill equations or more complex rational functions (Monod et al., 1965; Koshland et al., 1966; Cleland,

† This work was supported in part by U.S. Public Health Service Grant GM-30054 from the National Institutes of Health.
‡ Present address: Department of Biometry, Medical University of South Carolina, Charleston, SC 29425.

0006-2960/87/0426-6869$01.50/0 

1967) unmanageable (Savageau, 1972, 1976).

The intractability and ad hoc nature of models based on rational functions and the need for a more systematic description of organizationally complex systems have led us to take a fundamentally different approach, called the power-law formalism (Savageau, 1969a,b, 1970, 1971a,b, 1972). In this formalism, biochemical rate laws or other nonlinear functions are approximated by the constant plus linear terms of their Taylor series in logarithmic space. In Cartesian coordinates, this approximation yields a product of power-law functions.

There are alternative hierarchical levels at which biochemical systems can be described by this formalism (Savageau, 1969a,b, 1979, 1985a). The lowest level might correspond to the elemental chemical kinetic description for each of the steps in each of the enzyme-catalyzed reactions. At this level, the power-law description is exactly the same as that of conventional chemical kinetics [(Chapter 2 in Savageau (1976)]. The next level corresponds to the representation of individual enzyme-catalyzed reactions, for instance, by Michaelis–Menten or Hill rate laws or more complex functions. At this level, each reaction can be represented by a power-law function. If there are $p$ reactions that contribute to the increase of system component X and $q$ reactions that contribute to its decrease, then the change in X with time is represented by the sum of $p$ power-law functions representing increase minus the sum of $q$ power-law functions representing decrease (Savageau, 1969a,b). This is a common variant within the power-law formalism when systems of enzyme-catalyzed reactions are being considered. It gives rise to generalized mass-action equations. [A special case of this variant of the power-law formalism was adopted implicitly by Kacser and Burns (1973) and Heinrich and Rapoport (1974); for details, see Savageau et al. (1987a,b).] Another common variant results when one aggregates rate laws to obtain two functions, one representing the sum of the rate processes that lead to an increase in a given system constituent and the other representing the sum of the rate processes that lead to a decrease in that system constituent. Each of these aggregate rate laws is then represented by a single product of power-law functions. This variant gives rise to a set of equations called S systems, because of their ability to capture the synergistic and saturable properties that are characteristic of biological systems. This is the representation that was explicitly selected for the development of biochemical systems theory (Savageau, 1969b; Savageau et al., 1987a). At a higher level, one can aggregate system components, and the net rates of increase and decrease of these aggregate variables are again mathematical expressions that can be represented by power-law functions (Savageau, 1979). At a still higher level, one can describe the growth of organisms and their interactions at a biochemical level by means of this same power-law formalism (Savageau & Voit, 1982; Voit & Savageau, 1982a,b).

At each of these levels, comparisons with experimental data show that this power-law formalism is accurate over a surprisingly wide range of variation in concentrations in vivo [e.g., see Savageau (1976) and Voit and Savageau (1982a)].

The work described above raises two general questions: (1) Since there are alternative ways of representing the same phenomenon in this formalism, what is the relative accuracy of these alternatives? (2) Why is the power-law formalism so accurate?

We will approach the first of these general questions by focusing upon the more specific question, What is the relative accuracy of S-system and generalized mass-action equations in representing systems of enzyme-catalyzed reactions? This is equivalent to the question, What is the relative accuracy of aggregation to produce rate laws for individual enzyme-catalyzed reactions vs aggregation to produce rate laws for the net increase and net decrease of each system constituent?[1] We shall answer this question by determining the "range of validity" for both models, i.e., by determining the range of concentrations over which each power-law representation and the "actual" rate law differ by at most a given tolerance. The ideal reference for comparing these alternative strategies would be the "actual" rate laws for biochemical reactions in vivo. However, these rate laws are generally unknown, and we will instead consider Michaelis–Menten and Hill rate laws as references, with which we will compare both types of power-law models and the linear model. For simplicity, we will abbreviate Michaelis–Menten rate law as MMRL[2] and Hill rate law as HRL. Our results show that S-system equations, representing aggregation into rate laws for net increase and net decrease of system constituents, almost always improve the accuracy of the power-law representation.

$$X_1 \longrightarrow X_2$$

FIGURE 1: Essentially irreversible reaction in which substrate $X_1$ is used to form product $X_2$.

The second general question posed above, regarding the notable accuracy of the power-law representation, is discussed in the light of these results and others reported elsewhere.

## Power-Law Representation of Biochemical Rate Laws

### *Individual Reactions*

For simplicity, consider an essentially irreversible reaction in which substrate $X_1$ is used to form product $X_2$ (Figure 1). The rate of utilization of $X_1$ for the production of $X_2$ is denoted $v_{12}$ (lower-case $v$ for the rate of individual reactions), which in this instance is considered to be a function that depends only on the variable $X_1$. Following the established terminology in the power-law formalism (Savageau, 1969b), $v_{12}$ is represented by a power law in which $X_1$ is raised to a real power, the *apparent kinetic order*, and multiplied by a coefficient, the *apparent rate constant*. These two fundamental parameters are direct extensions of the kinetic order and rate constant of traditional biochemical kinetics. We use the symbols $g$ and $\alpha$ to represent these parameters in rate laws contributing to the increase in a given concentration and the symbols $h$ and $\beta$ to represent these parameters in rate laws contributing to the decrease in a given concentration. In our simple precursor–product relationship (although not in general), the rate of utilization of $X_1$ is mathematically identical with the rate of production of $X_2$, and we can write $v_{12}$ as

$$v_{12} = \beta_1 X_1^{h_{11}} \left(=-\frac{dX_1}{dt}\right)$$

or as

$$v_{12} = \alpha_2 X_1^{g_{21}} \left(=\frac{dX_2}{dt}\right)$$

depending on whether we focus on the utilization or on the production aspect of $v_{12}$. In this simple case, $\alpha_2 = \beta_1$ and $g_{21} = h_{11}$.

The parameters are determined by the well-known Taylor-series expansion [e.g., Thomas and Finney (1982)] of $v_{12}$

[1] Although these representations involve different levels of aggregation, we can, by restricting ourselves to just these two levels, say for simplicity that the former is the case *without* aggregation of rate laws while the latter is the case *with* aggregation of rate laws.

[2] Abbreviations: HRL, Hill rate law; MMRL, Michaelis–Menten rate law.

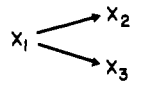


FIGURE 2: Diverging reactions. $X_1$ is a substrate that is converted via two routes to the products $X_2$ and $X_3$.

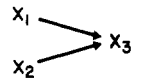


FIGURE 3: Converging reactions. The substrates $X_1$ and $X_2$ yield the same product, $X_3$.

in logarithmic space. However, it is not necessary to calculate the Taylor series explicitly; $h$ and $\beta$ (or $g$ and $\alpha$) can be derived directly from $v_{12}$ as (Savageau, 1971b)

$$h_{11} = \mathrm{d}(\log v_{12})/\mathrm{d}(\log X_1)|_{X_{10}} = (\mathrm{d}v_{12}/\mathrm{d}X_1)|_{X_{10}} X_{10}/[v_{12}(X_{10})]$$

$$\beta_1 = v_{12}(X_{10}) X_{10}^{-h_{11}}$$

where $X_{10}$ is the operating value for the Taylor-series expansion. These parameters are easily measured from experimental data in a log–log plot (Savageau, 1971b, 1976).

*Sums of Reactions*

Aggregation at the level of enzyme-catalyzed reactions (but not reactants) manifests itself only at points in a biochemical system where reactions converge to or diverge from a given constituent. Therefore, the impact of aggregation in a complex biochemical network can be approached by analyzing these two paradigm situations. Furthermore, we shall only consider two converging or diverging reactions; convergence or divergence of three or more reactions can be treated by successive aggregation of two reactions at a time.

In diverging pathways, a substrate $X_1$ is utilized via two different routes (Figure 2). The net rate of utilization of $X_1$ can be formulated as

$$V = v_{12} + v_{13}$$

where upper-case $V$ represents the net rate for these individual reactions. In the power-law formalism without aggregation, each reaction is represented by an individual power-law function. The first is equal to the rate of production of $X_2$, and the second is equal to the rate of production of $X_3$:

$$V = \alpha_2 X_1^{g_{21}} + \alpha_3 X_1^{g_{31}}$$

In contrast, the aggregation of both reactions that utilize $X_1$, $v_{12}$ and $v_{13}$, leads to one rate law for the net utilization of $X_1$ that is represented by one power-law function:

$$V = \beta_1 X_1^{h_{11}}$$

In converging pathways, two reactions yield the same product, $X_3$ (Figure 3). Without aggregation, the reactions for the utilization of the substrates $X_1$ and $X_2$ are represented by power-law functions, which together are equal to the net rate of production of $X_3$:

$$V = \beta_1 X_1^{h_{11}} + \beta_2 X_2^{h_{22}}$$

Whereas with aggregation, the net rate of production of $X_3$ is described by only one power-law term, and hence

$$V = \alpha_3 X_1^{g_{31}} X_2^{g_{32}}$$

The mathematical structure of these power-law descriptions is independent of the specific mathematical features of the actual rate laws. However, these features are reflected in the $\alpha$, $\beta$, $g$, and $h$ parameter values that are uniquely determined from the rate laws for the reactions. For the following, we will specify reactions that obey MMRL or HRL and study the quantitative effects of aggregation.

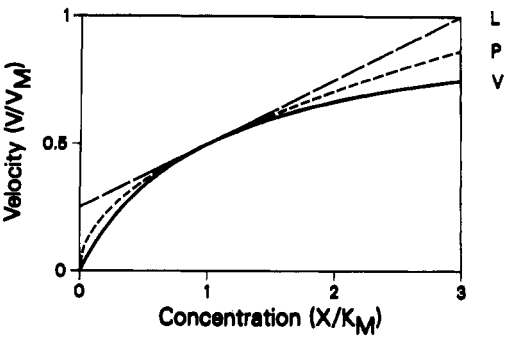


FIGURE 4: Individual Michaelis–Menten rate law. The actual rate law (V) and the corresponding power-law (P) and linear (L) representations are shown with $X_O = K_m$. Concentration and velocity are normalized with respect to $K_m$ and $V_m$, respectively.

## Power-Law Representation of Michaelis–Menten Rate Laws and Hill Rate Laws

We will consider individual rate laws first, because they provide information about the quality of the power-law and linear representations and hence will make analysis of results on diverging and converging pathways easier to understand.

*Individual Rate Laws*

In the usual nomenclature, the HRL is written

$$v = V_m X^n/(K_m^n + X^n)$$

where $v$ is the velocity of the reaction or the rate of product formation, $V_m$ is the maximum velocity, $X$ is the substrate concentration, $K_m$ is equal to the substrate concentration that produces half the maximum velocity, and $n$ is called the "Hill coefficient". If $n = 1$, $v$ is the MMRL. The general HRL ($n \neq 1$) is a reasonable representation of the kinetics for many allosteric enzymes (Atkinson, 1966). Many kinetic studies indicate that $n$ usually lies between 1 and 2 and rarely if ever exceeds 4.

The power-law representation of $v$ is

$$v_P = \alpha X^g$$

where the parameters $\alpha$ and $g$ are calculated as shown before:

$$g = nK_m^n/(K_m^n + X_O^n)$$

which reduces for the MMRL to

$$g = K_m/(K_m + X_O)$$

and

$$\alpha = v(X_O) X_O^{-g}$$

which has the same form for both MMRL and the HRL but, in general, a different value.

Besides the parameters $V_m$, $K_m$, and $n$ that underlie both $v$ and $v_P$, $v_P$ involves the operating value $X_O$. Many enzymes are considered to operate around their $K_m$ under physiological conditions, and if little is known about the real system under invstigation, $X_O = K_m$ is often a good initial choice. Figure 4 shows a plot of a MMRL and the corresponding power-law representation. $v_P$ and $v$ are equal at $X = 0$ and $X = X_O$; otherwise, $v_P$ always overestimates $v$. Furthermore, because $v$ and $v_P$ are always concave downward, $v_P$ is globally a better representation than the linear representation

$$v_L = v(X_O) + \mathrm{d}v/\mathrm{d}X|_{X_O} \cdot (X - X_O)$$

The accuracy of $v_P$ can be measured by the relative error $E = (v_P - v)/v$. $E$ depends on the relationship between $X_O$

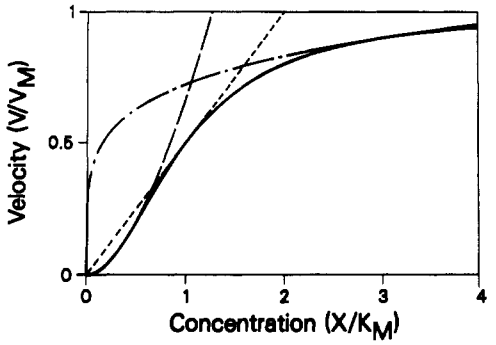


FIGURE 5: Individual Hill rate law. The Hill coefficient is $n = 2$, the critical concentration $X_C = K_m$, and the inflection point $X_I = 0.577K_m$. Three power-law representations are shown: $X_O = 0.4K_m$ (--), $X_O = K_m$ (---), and $X_O = 3K_m$ (---).

and $K_m$ but not on $V_m$. The range of concentrations for which this error is less than a specified tolerance can be calculated by numerically inverting $E(X)$ for given $X_O$ and $K_m$ or can be obtained graphically from a plot of $E$ vs $X$.

In contrast to the MMRL, whose graph is always concave downward and so has no inflection, the HRL is S-shaped with zero slopes for $X \rightarrow 0$ and $X \rightarrow \infty$, if $n > 1$. Depending on the relation between the operating value $X_O$ and the critical value $X_C = K_m(n-1)^{1/n}$, $v_P$ is either concave upward ($X_O < X_C$), a straight line ($X_O = X_C$), or concave downward ($X_O > X_C$) (Figure 5). At $X_C$, the tangent to $v$ goes through the origin, and $v_P$ is then identical with the linear representation $v_L$. In contrast to the MMRL, where $v_P$ is globally better than $v_L$ (see Figure 4), the superiority of one or the other representation of the HRL depends on the value of $X_O$ (see Figure 5). If $X_O > X_C$, $v_P$ is globally better. This can best be seen from the plots of $v$, $v_P$, and $v_L$ in logarithmic coordinates: log $v$ corresponds to a concave function facing downward, log $v_P$ to a straight line, and log $v_L$ to a concave function facing upward. All three touch at $X_O$ (Figure 6a). If $X_O$ lies between the inflection point $X_I = K_m[(n-1)/(n+1)]^{1/n}$ and $X_C$ ($X_I \leq X_O < X_C$), then $v_L$ is superior to $v_P$ because $v$ and $v_P$ are concave downward and upward, respectively, and are separated by $v_L$. For $X_O < X_I$, either one of the representations $v_L$ or $v_P$ can be superior, depending on the parameter values in the rate law and on the direction of deviation from the operating point, as illustrated in Figure 6b.

*Sums of Rate Laws*

*Diverging Reactions Described by MMRL.* If $X$ (=$X_1$) is used for the production of $X_2$ and $X_3$, as sketched in the general section above, its utilization via two MMRL is represented mathematically as

$$V = v_{12} + v_{13} = V_{m2}X/(K_{m2} + X) + V_{m3}X/(K_{m3} + X)$$

The corresponding power-law representations $V_{P+}$ (with aggregation) and $V_{P-}$ (without aggregation) for this type of utilization are

$$V_{P+} = \beta X^h$$

and

$$V_{P-} = \alpha_2 X^{g_2} + \alpha_3 X^{g_3}$$

For simplicity, all indices have been reduced here to the necessary minimum.

At first glance, $V_{P+}$ might seem to be a special case of $V_{P-}$ with $\beta = \alpha_2$, $h = g_2$, and $\alpha_3 = 0$. However, the parameters $\beta$, $h$, $\alpha_2$, $\alpha_3$, $g_2$, and $g_3$ in $V_{P+}$ and $V_{P-}$ cannot be chosen freely to yield the optimal representation of $V$ but are uniquely derived from the Taylor-series expansions of $V$, $v_{12}$, and $v_{13}$.

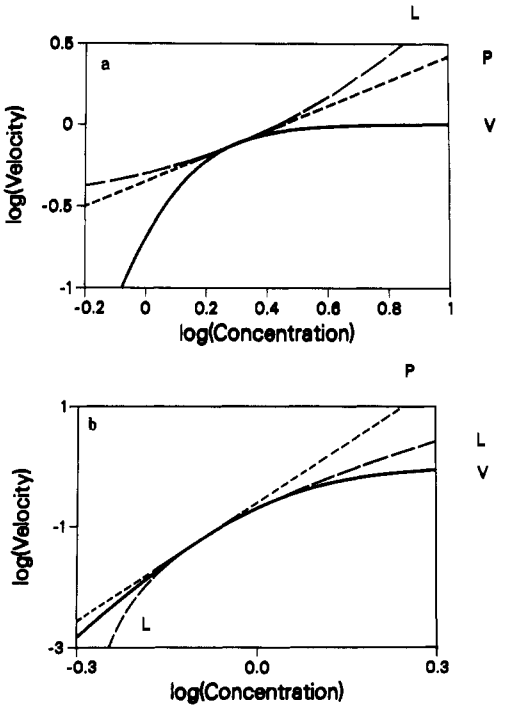


FIGURE 6: Individual Hill rate law. The actual rate law (V) and the corresponding power-law (P) and linear (L) representations are shown in logarithmic space. The relevant parameters are (a) $n = 3$, $X_I = 0.79K_m$, $X_C = 1.26K_m$, and $X_O = 2K_m$ and (b) $n = 4$, $X_I = 0.88K_m$, $X_C = 1.32K_m$, and $X_O = 0.2K_m$.

In particular, $\alpha_2 X^{g_2}$ represents $v_{12}$ exclusively and has no influence on the representation of $v_{13}$. In contrast, $\beta$ and $h$ depend on all parameters in $V$ simultaneously, which often leads to an improved representation of $V$, as we will see later.

The parameters in $V_{P+}$ and $V_{P-}$ are

$$h = \{V_{m2}K_{m2}(K_{m3} + X_O)^2 + V_{m3}K_{m3}(K_{m2} + X_O)^2\}/\{(K_{m2} + X_O)(K_{m3} + X_O)[V_{m2}(K_{m3} + X_O) + V_{m3}(K_{m2} + X_O)]\}$$

$$\beta = V(X_O)X_O^{-h}$$

and

$$g_2 = K_{m2}/(K_{m2} + X_O)$$

$$\alpha_2 = v_{12}(X_O)X_O^{-g_2}$$

$$g_3 = K_{m3}/(K_{m3} + X_O)$$

$$\alpha_3 = v_{13}(X_O)X_O^{-g_3}$$

The superiority of either representation can often be shown by studying $V$, $V_{P+}$, $V_{P-}$, and $V_L$ in logarithmic coordinates, that is, by analyzing log $V$, log $V_{P+}$, log $V_{P-}$, and log $V_L$ as a function of log $X$. The log $V_{P-}$ is always above the straight lines given by log $\alpha_2$ + $g_2$ log $X$ and log $\alpha_3$ + $g_3$ log $X$, which it approaches as $X$ goes to zero or infinity. The log $V_{P+}$ corresponds to a straight line with slope $h$ and intercept log $\beta$. Its slope is a weighted average of the slopes $g_2$ and $g_3$ for the asymptotes of log $V_{P-}$ and hence always lies between them:

$$h = \frac{g_2 v_{12}(X_O) + g_3 v_{13}(X_O)}{v_{12}(X_O) + v_{13}(X_O)}$$

The log $V_L$ is, like log $V_{P-}$, concave upward but, because of its greater curvature, always lies above log $V_{P-}$. For all relevant parameter values, log $V$ produces lower values than log $V_{P+}$ and, because all four functions have the same value and the same slope at $X_O$, $V_{P+}$ is the best representation of $V$, and $V_{P-}$ is better than $V_L$ (cf. Figure 7). Only if $K_{m2}$ and $K_{m3}$ differ by several orders of magnitude will particular combinations

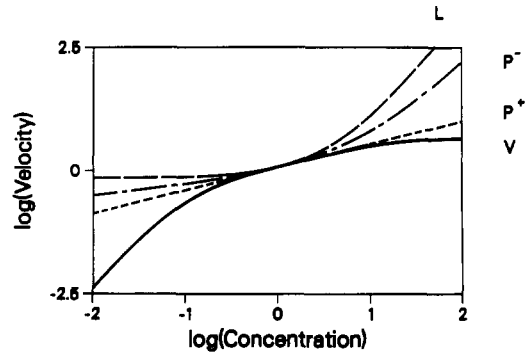


FIGURE 7: Sum of two Michaelis–Menten rate laws describing diverging reactions. The actual rate law (V), the power-law representations with (P+) and without (P–) aggregation, and the linear representation (L) are shown in logarithmic space. The relevant parameters are $V_{m2} = V_{m3} = 1$, $K_{m2} = 0.1$, $K_{m2} = 5$, and $X_O = 1$.

of $V_{m2}$, $V_{m3}$, and $X_O$ yield superiority of either $V_{P-}$ or $V_L$; this case can be quantified with the methods of the next section and is discussed there.

The ranges of validity, within which the differences between $V_{P+}$, $V_{P-}$, or $V_L$ and $V$ are less than a given tolerance, depend on the numerical values of the parameters in $V$ and the operating value for $X$.

*Diverging Reactions Described by HRL.* A pathway with two diverging reactions, each represented by a HRL, can be expressed mathematically as

$$V = v_{12} + v_{13} = V_{m2}X^{n_2}(K_{m2}{}^{n_2} + X^{n_2}) + V_{m3}X^{n_3}(K_{m3}{}^{n_3} + X^{n_3})$$

The corresponding power-law representations with and without aggregation have the same form as for two diverging MMRL; their parameter values are calculated analogously and include the Hill coefficients $n_2$ and $n_3$.

The shape of the graph of $V$ vs $X$ depends on all the numerical relationships among the parameter values in $V$ but mainly on the ratio of the $K_m$ values: Two $K_m$ values that are about equal yield a sigmoid graph similar to that of a single HRL, whereas a large ratio of $K_m$ values produces a pronounced double-sigmoid shape (Figure 8a,b). The graph of log $V$ in this case is characterized by the asymptotes and breakpoints of log $V$ [Appendix A of Savageau (1976)] and reflects the transition from dominance by the first HRL to that by the second (Figure 8c). The consequence of the indentation is that any of the three representations, $V_L$, $V_{P+}$, or $V_{P-}$, can be best, depending on the value of the operating point. As in the case of two MMRL, $V_{P-}$ is always concave upward, and $V_{P+}$ is a straight line in logarithmic coordinates. $V_L$ in logarithmic coordinates is either concave upward, straight, or concave downward, if its constant term in Cartesian coordinates is positive, zero, or negative, respectively. Such topological considerations often yield a qualitative comparison. For instance, they show that, depending on the operating value, $V_{P-}$ can have the correct curvature (in Figure 8c for operating value log $X_O = 0.75$) or the wrong curvature (in Figure 8c for log $X_O = -0.75$ or log $X_O = 1.5$).

A quantitative comparison between $V_{P+}$, $V_{P-}$, or $V_L$ and $V$ shows that the superiority of any of the three representations depends on the numerical values for the six parameters in $V$ and on the value of $X_O$. The large number of parameters and, hence, of possible combinations of parameter values and operating points yields an enormous number of quantitatively different results. This situation has influenced us to develop a more global measure for the superiority of a representation. We assume that the substrate concentration can deviate from

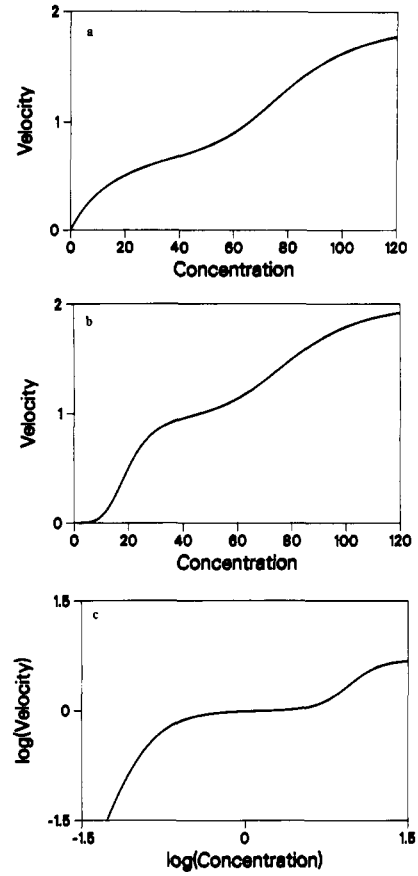


FIGURE 8: Sum of two Hill rate laws describing diverging reactions. (a) and (b) are in Cartesian coordinates; (c) is in logarithmic coordinates. The values for the parameters $n_2$, $V_{m2}$, $K_{m2}$, $n_3$, $V_{m3}$, and $K_{m3}$ are as follows: (a) 1, 20, 1, 6, 80, and 50; (b) 4, 20, 1, 6, 80, and 50; (c) 2, 1, 0.1, 3, 1, and 10.

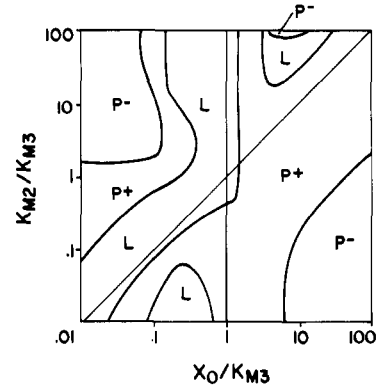


FIGURE 9: Comparison of accuracy for the sum of two Hill rate laws describing diverging reactions. The accuracy of representation at each point depends on the ratio of Michaelis constants ($K_{m2}/K_{m3}$) and the ratio of the operating value to one of the Michaelis constants ($X_O/K_{m3}$). The most accurate representation within each region is indicated by the symbols P+ (power-law representation with aggregation), P– (power-law representation without aggregation), or L (linear representation). The most relevant region is bound by the vertical and diagonal lines, in which the operating value is between the $K_m$ values. The scales are logarithmic; the relevant parameter values are $V_{m2} = V_{m3} = 1$, $n_2 = 2$, and $n_3 = 4$. See text for further discussion.

the operating point up to a given degree. The average absolute difference between a representation and the HRL within this range then yields a measure for the superiority of one of the representations for given parameter values and a given operating point. Figure 9 shows for the different representations how such regions of superiority depend on the $K_m$ values and the operating point $X_O$, while the remaining parameter values are fixed. For the results in Figure 9 we assumed that the

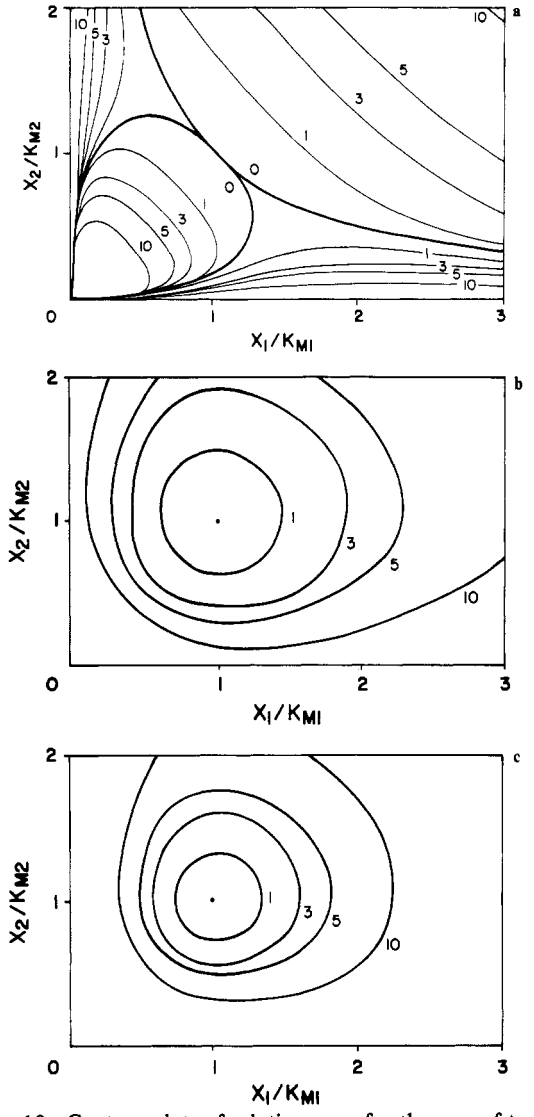


FIGURE 10: Contour plots of relative error for the sum of two Michaelis–Menten rate laws describing converging reactions. Errors are shown as the percentage difference between the actual rate law and (a) the power-law representation with aggregation, (b) the power-law representation without aggregation, and (c) the linear representation. Substrate concentrations are normalized with respect to the appropriate $K_m$ value; the maximum velocities are $V_{m1} = V_{m2} = 1$. See text for discussion.

substrate concentration can deviate ±10-fold for $X_O$. This logarithmic deviation from $X_O$ is generally more appropriate than a linear deviation (Savageau, 1971b). However, the regions of superiority only change minimally if the substrate concentration varies within a smaller range or if the deviations from $X_O$ are assumed linear. If the parameter values in $V$ are chosen differently, the results still are topologically similar to those in Figure 9, although the regions of superiority move slightly and become smaller or larger.

In all cases, aggregation improves the quality of the power-law representation over the most relevant region, namely, that bounded by the vertical and diagonal lines, in which the operating point is between the $K_m$ values (Figure 9). Within this region, the power-law representation with aggregation is more accurate than that without aggregation. However, if the ratio of the $K_m$ values is large, then the power-law representation without aggregation can be superior (Figure 9). A large ratio would mean that the reaction with the lower $K_m$ reaches its maximal velocity at low substrate concentrations, while there is very little flux through the other reaction.[3]

In contrast to diverging MMRL, the linear approximation to diverging HRL is sometimes more accurate than either power-law representation.

*Converging Reactions Described by MMRL.* The rate of formation of a product from two substrates $X_1$ and $X_2$ via independent converging routes can be written as

$$V = v_{13} + v_{23} = V_{m1}X_1/(K_{m1} + X_1) + V_{m2}X_2/(K_{m2} + X_2)$$

This equation looks similar to the previous equation for diverging MMRL, but we are now dealing with two variables, $X_1$ and $X_2$. The corresponding approximations with simplified indices are

$$V_{P+} = \alpha X_1^{g_1} X_2^{g_2}$$

and

$$V_{P-} = \beta_1 X_1^{h_1} + \beta_2 X_2^{h_2}$$

where the parameters are calculated from $V$ as shown before:

$$g_1 = \frac{V_{m1}K_{m1}(K_{m2} + X_{20})X_{10}}{(K_{m1} + X_{10})[V_{m1}X_{10}(K_{m2} + X_{20}) + V_{m2}X_{20}(K_{m1} + X_{10})]}$$

$$g_2 = \frac{V_{m2}K_{m2}(K_{m1} + X_{10})X_{20}}{(K_{m2} + X_{20})[V_{m1}X_{10}(K_{m2} + X_{20}) + V_{m2}X_{20}(K_{m1} + X_{10})]}$$

$$\alpha = V(X_{10},X_{20})X_{10}^{-g_1}X_{20}^{-g_2}$$

$$h_1 = K_{m1}/(K_{m1} + X_{10})$$

$$\beta_1 = v_{13}(X_{10})X_{10}^{-h_1}$$

$$h_2 = K_{m2}/(K_{m2} + X_{20})$$

$$\beta_2 = v_{23}(X_{20})X_{20}^{-h_2}$$

As in the previous example with diverging pathways, $V_{P-}$ contains more parameters, but again, since the parameters cannot be chosen freely, the larger number does not necessarily lead to a better representation for $V$.

The straightforward approach to comparing $V_{P+}$, $V_{P-}$, or $V_L$ and $V$ would be analysis of the error functions $E_1 = (V - V_{P+})/V$, $E_2 = (V - V_{P-})/V$, or $E_3 = (V - V_L)/V$ and, specifically, determination of their maxima, minima, and zeroes. Unfortunately, such an analysis leads to conditions for the superiority of one or the other representation that contain the system variables and parameters in a complicated manner that yields little insight. An indication of the mathematical complexity can be gained from the solutions to the equations $E_1$

[3] Unfortunately, it is difficult to find appropriate experimental data to decide whether the $K_m$ values for divergent reactions in vivo are similar or different. Similar $K_m$ values have been determined for the enzymes in *Escherichia coli* that use aspartate as substrate: aspartokinases I, II, and III [$K_m$ between 1 and 5 mM (Truffa-Bachi & Cohen, 1966; Patte et al., 1967)], asparagine synthetase [$K_m$ = 0.8 mM (Cedar & Schwartz, 1969)], and aspartate transcarbamylase [$K_m$ = 6 mM (Weitzman & Wilson, 1966)]. Similar $K_m$ values also have been found for the enzymes prephenate dehydratase [$K_m$ = 0.47 mM (Duggleby et al., 1978)] and prephenate dehydrogenase [$K_m$ = 0.37 mM (Koch et al., 1971)] that use prephenate as substrate. In contrast to these examples, the $K_m$ values seem to differ considerably for enzymes that use chorismate as substrate: anthranilate synthetase [$K_m$ between 0.0012 and 0.0055 mM (Baker & Crawford, 1966; Ito & Yanofsky, 1969; Pabst et al., 1973) for *E. coli*; $K_m$ = 0.0037 mM for *Salmonella typhimurium* (Henderson et al., 1970)], chorismate mutase/prephenate dehydrogenase [$K_m$ = 0.39 mM (Koch et al., 1971) in *E. coli*], chorismate mutase/prephenate dehydratase [$K_m$ between 0.024 and 0.045 mM in *E. coli* (Duggleby et al., 1978; Dopheide et al., 1972) and between 0.08 and 0.12 mM in *S. typhimurium* (Schmidt & Zalkin, 1969, 1971; Schmidt et al., 1970)]. Interpreting such experimental data is difficult because most of these enzymes are regulated in vivo by other metabolites, which can result in effective $K_m$ values very different from those measured in vitro.

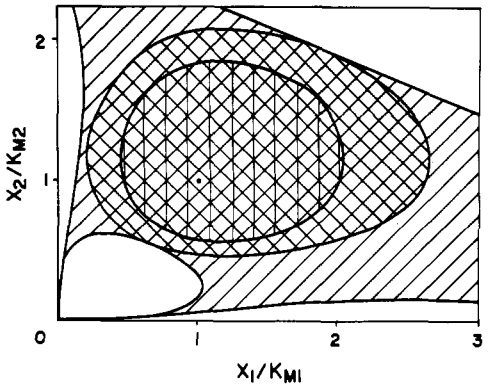


FIGURE 11: Range of validity about an operating point for the sum of two Michaelis–Menten rate laws describing converging reactions. The range of concentration values for which the deviations from the actual rate law are less than 5% is indicated for the power-law representations with (///) and without (\\\) aggregation and for the linear representation (|||). Substrate concentrations are normalized with respect to the appropriate $K_m$ value; the maximal velocities are $V_{m1} = 0.9$ and $V_{m2} = 1.3$; the operating point is (1, 1), which corresponds to ($X_{10} = K_{m1}$, $X_{20} = K_{m2}$).

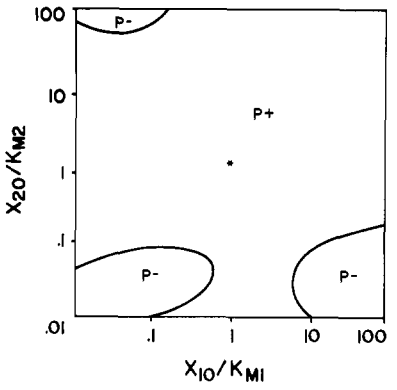


FIGURE 12: Comparison of accuracy at different operating points for the sum of two Michaelis–Menten rate laws describing converging reactions. The most accurate representation within each region is indicated by the symbols P+ (power-law representations with aggregation) and P– (power-law representation without aggregation). The operating values for the substrate concentrations are normalized with respect to the relevant $K_m$ value and represented on logarithmic scales. The maximal velocities are $V_{m1} = 3$ and $V_{m2} = 8$. The symbol (*) indicates operation about the $K_m$ values. The linear representation is always inferior.

$= 0$, $E_2 = 0$, or $E_3 = 0$, which correspond to points of identity between $V$ and $V_{P+}$, $V$ and $V_{P-}$, or $V$ and $V_L$, and from contour plots, which consist of lines of constant relative error between $V$ and one of the representations ($E_1$ = constant, $E_2$ = constant, or $E_3$ = constant; panels a–c of Figure 10). $V_{P+}$ represents $V$ exactly at an infinite number of concentration pairs ($X_1/K_{m1}$, $X_2/K_{m2}$) that lie on an irregularly shaped curve. The contour lines ($E_1$ = constant) are "parallel" to this curve. $V_{P-}$ is only equal to $V$ the origin and the operating point; its contour lines are centered around the operating point and are more or less round or elliptical (Figure 10b). The linear representation $V_L$ produces contour lines that roughly parallel those of $V_{P-}$, but the ranges of validity for $V_L$ are considerably smaller and always completely inside those for $V_{P-}$ (Figure 10b,c).

In Figure 11, the range of validity with less than 5% error is shown for $V_{P+}$, $V_{P-}$, and $V_L$. The range of validity for $V_{P+}$ is much wider and completely[4] includes that for $V_{P-}$ as long as the operating values are greater than or equal to the corresponding $K_m$ values. If the operating values are smaller than the $K_m$ values, $V_{P+}$ can still be superior. However, if at least one of the operating values is sufficiently small, then $V_{P-}$ can be better than $V_{P+}$ for some substrate concentrations below that operating value. For other operating points and other error tolerances, the ranges of validity have a topology similar to that in Figure 11, although their borders are numerically different.

In cases, where one operating value is small and hence the range of validity for $V_{P+}$ does not completely include the range for $V_{P-}$, the overall quality of $V_{P+}$ and $V_{P-}$ is difficult to judge. For some concentrations, $V_{P+}$ is better and for other concentrations $V_{P-}$. Furthermore, $V_{P-}$ always yields a compact, more or less round or elliptical, range around the operating point, whereas the range for $V_{P+}$ is larger but more irregular in shape. In this graphical comparison, the superiority of one or the other representation can be ambiguous and may depend not only on the distance from the operating point but also on the direction in which the system is perturbed from the operating point.

Another way of comparing $V_{P+}$, $V_{P-}$, and $V_L$ results if one assumes that perturbations from the operating point occur in all directions with the same probability and then compares the average error for a given extent of perturbation. In mathematical terms, one averages the differences between $V$ and $V_{P+}$, $V$ and $V_{P-}$, or $V$ and $V_L$ over all directions within a given distance from ($X_{10}/K_{m1}$, $X_{20}/K_{m2}$). It is appropriate to consider logarithmic perturbations say from $K_m$ to $(1/2)K_m$ and from $K_m$ to $2K_m$ (Savageau, 1971b). A measure for the validity of a given representation at a specific operating point is then the average error for all perturbations up to a given extent. Other types of perturbation also could be used, and the conclusions are unchanged.

This kind of comparison clearly shows the superiority of $V_{P+}$ over $V_{P-}$ and of both power-law representations over $V_L$, which is nowhere best (Figure 12). Although there are regions in which $V_{P-}$ produces smaller average errors than $V_{P+}$, a wide region around the point (1, 1), which represents operation at the $K_m$ values, is dominated by $V_{P+}$. Since this region is the relevant one for most real biochemical systems, $V_{P+}$ has to be considered better than $V_{P-}$.

Quantitatively, the borders between the regions of $V_{P+}$ superiority and $V_{P-}$ superiority are only slightly dependent on the largest possible perturbation and on possible weights associated with perturbations of a given extent, e.g., small perturbations may be more probable than large perturbations. However, for wide variations in these conditions we have found that the borders in Figure 12 change only insignificantly. The borders also depend on the parameter values in $V$, but again, the topology in Figure 12 is not changed. If $V_{m1}$ and $V_{m2}$ are equal, then Figure 12 becomes symmetrical about the diagonal; if $V_{m1}$ and $V_{m2}$ are different, the regions are systematically distorted as in Figure 12. Figure 12 therefore basically covers the whole spectrum of parameter values in $V$.

The power-law representations $V_{P+}$ and $V_{P-}$ are always globally better than the linear representation $V_L$. This is a special feature of the MMRL and is no longer true if the MMRL is replaced by the HRL with Hill coefficients greater than 1, as we will see next.

*Converging Reactions Described by HRL.* If a product is formed via two independent converging reactions that are described by HRL, then the rate of formation of product is

$$V = v_{13} + v_{23} = V_{m1}X_1^{n_1}/(K_{m1}^{n_1} + X_1^{n_1}) + V_{m2}X_2^{n_2}/(K_{m2}^{n_2} + X_2^{n_2})$$

The mathemtaical forms of the power-law representations with

[4] This statement is true for all substrate concentrations of interest. If one of the substrate concentrations is almost zero, $V_{P-}$ represents $V$ better than $V_{P+}$. However, these ranges along the axes are so slim that they cannot be shown with the resolution of Figure 11.

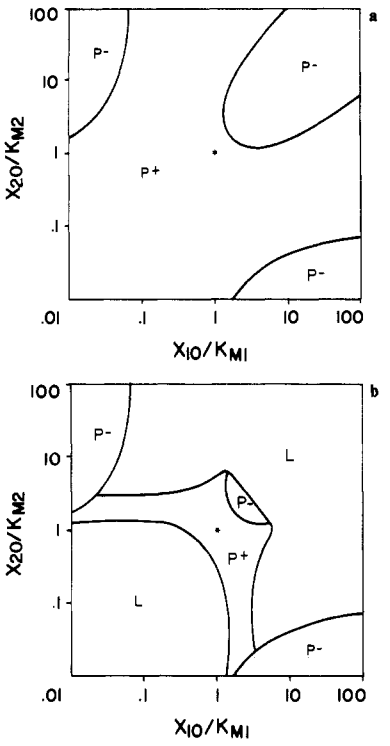


FIGURE 13: Comparison of accuracy at different operating points for the sum of two Hill rate laws describing converging reactions. (a) The most accurate representation within each region is indicated by the symbols P+ (power-law representation with aggregation) and P– (power-law representation without aggregation). The relevant parameters are $n_1 = 2$, $V_{m1} = 1$, $n_2 = 2$, and $V_{m2} = 1$. The operating values for the substrate concentrations are normalized with respect to the relevant $K_m$ value and represented on logarithmic scales. The symbol (*) indicates operation about the $K_m$ values. Panel b is the same as panel a except that the linear representation is included in the comparisons; its regions of superiority are indicated by the symbol L.

and without aggregation are the same as for two MMRL, but their parameters are functions of the Hill coefficients $n_1$ and $n_2$:

$$g_1 = V_{m1}n_1X_{10}^{n_1}(K_{m2}^{n_2} + X_{20}^{n_2})/\{(K_{m1}^{n_1} + X_{10}^{n_1}) \times [V_{m1}X_{10}^{n_1}(K_{m2}^{n_2} + X_{20}^{n_2}) + V_{m2}X_{20}^{n_2}(K_{m1}^{n_1} + X_{10}^{n_1})]\}$$

$$g_2 = V_{m2}n_2X_{20}^{n_2}(K_{m1}^{n_1} + X_{10}^{n_1})/\{(K_{m2}^{n_2} + X_{20}^{n_2}) \times [V_{m2}X_{20}^{n_2}(K_{m1}^{n_1} + X_{10}^{n_1}) + V_{m1}X_{10}^{n_1}(K_{m2}^{n_2} + X_{20}^{n_2})]\}$$

$$\alpha = V(X_{10},X_{20})X_{10}^{-g_1}X_{20}^{-g_2}$$

$$h_1 = n_1/(K_{m1}^{n_1} + X_{10}^{n_1})$$

$$\beta_1 = v_{13}(X_{10})X_{10}^{-h_1}$$

$$h_2 = n_2/(K_{m2}^{n_2} + X_{20}^{n_2})$$

$$\beta_2 = v_{23}(X_{20})X_{20}^{-h_2}$$

The comparison of $V_{P+}$ and $V_{P-}$ with respect to average errors after perturbation shows that $V_{P+}$ represents $V$ better than $V_{P-}$ for wide variations of operating values below and around the $K_m$ values, whereas $V_{P-}$ is only superior to $V_{P+}$ for operating points greater than both $K_m$ values. In this latter range, the linear representation is usually better than either power-law representation (Figure 13). Although the Hill coefficients $n_1$ and $n_2$ influence the borders of the regions in which one or the other representation is superior, the topology is unchanged.

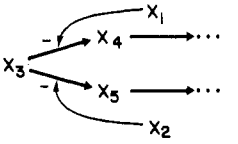


FIGURE 14: Modulation of diverging reactions. $X_3$ is the common substrate, $X_1$ and $X_2$ are allosteric inhibitors, $X_4$ and $X_5$ are intermediates in the diverging pathways.

In contrast to the case with two converging MMRL, the linear representation

$$V_L = V(X_{10},X_{20}) + (X_1 - X_{10})V_{m1}n_1X_{10}^{n_1-1}/(K_{m1}^{n_1} + X_{10}^{n_1})^2 + (X_2 - X_{20})V_{m2}n_2X_{20}^{n_2-1}/(K_{m2}^{n_2} + X_{20}^{n_2})^2$$

can be more accurate than either power-law representation. An example is shown in Figure 13b.

*Modulation of Enzyme-Catalyzed Reactions*

Production and utilization of many metabolites in vivo are regulated by other metabolites, which, under physiological conditions, assures that each flux and metabolite is maintained at the appropriate level. The modulation of the production of a metabolite $X_i$ by another metabolite $X_j$ is represented in power-law formalism by including $X_j$, raised to a power $g_{ij}$, in the positive term for the change in $X_i$. The modulation of utilization corresponds to the analogous inclusion of $X_j$, raised to a power $h_{ij}$, in the negative term for the change in $X_i$. The parameters $g_{ij}$ and $h_{ij}$ are positive kinetic orders if the modulation is an activation, and they are negative for inhibition.

With respect to analyzing the impact of aggregation, the power-law representations with and without aggregation differ only if modulation takes place at converging or diverging reactions. The most common type is inhibition at diverging reactions, which allows the cell to channel the flow of material into one or the other branch of the metabolic network according to current requirements. The schematic diagram for this type of inhibition (Figure 14) illustrates the flow of material (arrows between metabolites) and the modulations (arrows from metabolites to the center of an arrow); the minus sign next to an arrowhead indicates that the modulation is an inhibition [for further discussion of these conventions, see Savageau (1976) and Voit and Savageau (1982b)]. $X_1$ and $X_2$ may or may not be direct products of the diverging pathways starting at $X_3$.

Experimental observations indicate that such modulations follow sigmoidal kinetics; thus, the influence of $X_1$ and $X_2$ can be written

$$V = v_{34} + v_{35} = c_1/(K_{I1}^{n_1} + X_1^{n_1}) + c_2/(K_{I2}^{n_2} + X_2^{n_2})$$

if $X_3$ is kept constant. $c_1$ and $c_2$ are constants that include the fixed concentration of $X_3$. Without loss of generality, $X_1$ and $X_2$ can be scaled with respect to their $K_I$ values, and $c_1$ can be made equal to 1 by appropriately scaling time.

The power-law representations with ($V_{P+}$) and without ($V_{P-}$) aggregation for the modulated utilization of $X_3$ read, with slight simplification of notation

$$V_{P+} = \beta X_1^{h_1}X_2^{h_2}$$

and

$$V_{P-} = \alpha_1X_1^{g_1} + \alpha_2X_2^{g_2}$$

where the parameters are

$$h_1 = -n_1X_{10}^{n_1}(1 + X_{20}^{n_2})/[(1 + X_{10}^{n_1}) \times (1 + X_{20}^{n_2}) + c_2(1 + X_{10}^{n_1})^2]$$

$$h_2 = -n_2 X_{20}^{n_2}(1 + X_{10}^{n_1})/[(1 + X_{20}^{n_2}) \times (1 + X_{10}^{n_1}) + (1 + X_{20}^{n_2})^2]$$

$$\beta = V(X_{10}, X_{20}) X_{10}^{-h_1} X_{20}^{-h_2}$$

$$g_1 = -n_1 X_{10}^{n_1 - 1}/(1 + X_{10}^{n_1})$$

$$g_2 = -n_2 X_{20}^{n_2 - 1}/(1 + X_{20}^{n_2})$$

$$\alpha_1 = v_{34}(X_{10}) X_{10}^{-g_1}$$

$$\alpha_2 = v_{35}(X_{20}) X_{20}^{-g_2}$$

The representations were compared with respect to average errors after perturbation from the operating point, as outlined for two converging reactions described by MMRL, and similar results were obtained. $V_{P+}$ is superior to $V_{P-}$ because it always produces smaller errors for a wide range of variation in operating values around the corresponding $K_I$ values, no matter what the specific values for the parameters are (Figure 15a). For the same reasons, $V_{P+}$ is also superior to $V_L$, as long as the Hill coefficients are close to 1 (Figure 15a). For larger Hill coefficients, the picture becomes more complicated, and either $V_{P+}$ or $V_L$ can be best within the relevant region around the $K_I$ values, whereas $V_{P-}$ is the best representation only for less relevant operating points (Figure 15b).

From the form of the last two power-law equations it is clear that the analysis of converging reactions would give identical results. Similarly, activation of converging or diverging reactions would be analyzed exactly as converging reactions were in the previous sections, and the same results would be obtained.

## Discussion

The inherently complex nature of biochemical systems in vivo requires description and analysis in a mathematical language. Three distinct types of formalisms have been used for describing biochemical systems: (1) the Michaelis–Menten formalism, (2) the linear formalism, and (3) the power-law formalism.

By the term Michaelis–Menten formalism we do not mean just the original Michaelis–Menten assumptions, derivation, and specific rate law (Michaelis & Menten, 1913) but the broader spectrum of subsequent developments in enzyme kinetics that nonetheless share key assumptions and empirical methodology (Monod et al., 1965; Koshland et al., 1966; Cleland, 1967). For example, the assumption that there are no interactions between the various enzyme forms in a mechanism or between forms from other enzymes yields steady-state equations that are linear in the concentration variables for the enzyme forms (Cleland, 1967). The solution of these equations produces rate laws that are rational functions in the concentrations of the relevant reactants and modifiers and that are linearly related to the concentration of total enzyme (Wong & Hanes, 1962; Savageau, 1969a). The Michaelis–Menten formalism has significantly influenced biochemistry, and symbols like $K_m$ and $V_m$ have become a standard. Michaelis–Menten rate laws are almost considered as reality. One reason for their success is testability in vitro and the data showing that, under appropriate conditions, they provide a good approximation to the rate law for many isolated enzyme-catalyzed reactions. Nevertheless, the Michaelis–Menten formalism has serious disadvantages. (1) There is abundant evidence that enzyme forms can and do associate to form complexes in vivo as well as in vitro [see Welsh (1987) and Savageau et al. (1987a)]. For such systems, the rate laws need not be rational functions, nor must the rate laws be linearly related to total enzyme concentration. Such enzymes fall outside the realm of the Michaelis–Menten formalism. (2) Assuming that the formalism were valid, there are difficulties with the amount of experimental data necessary to determine kinetically the rate law for many mechanisms (Savageau, 1972, 1976). (3) Even if the data were available, there is no generally accepted method of enzyme kinetic analysis with which one can extract the relevant parameter values from the experimental data when double-reciprocal plots are nonlinear (Cleland, 1967). [However, see pp 74–76 of Savageau (1976).] (4) As soon as one considers complex biochemical systems in which several reactions participate, the mathematics in the Michaelis–Menten formalism become intractable (Savageau, 1972), and features of the integrated biochemical system, such as stability, oscillations, and sensitivity to changes in individual constituents, are very difficult to predict.

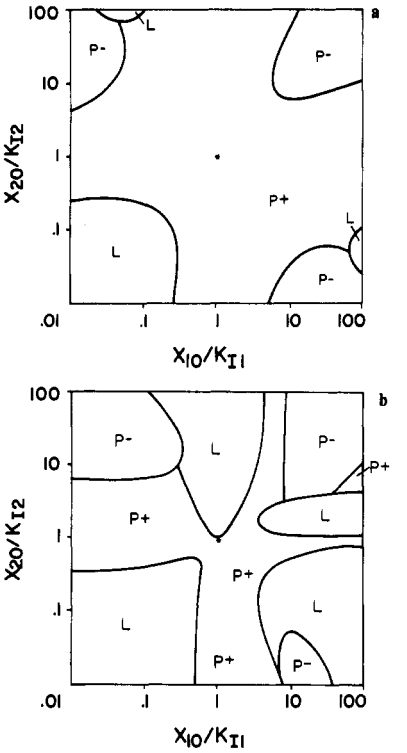


FIGURE 15: Comparison of accuracy at different operating points for the sum of two modulated Hill rate laws describing diverging reactions. The most accurate representation within each region is indicated by the symbol P+ (power-law representation with aggregation), P– (power-law representation without aggregation), or L (linear representation). The operating values for the inhibitor concentrations are normalized with respect to the relevant $K_I$ values and represented on logarithmic scales. The symbol (*) indicates operations about the $K_I$ values. The Hill coefficients are (a) $n_1 = n_2 = 1$ and (b) $n_1 = 2$ and $n_2 = 4$.

The mathematical complexity of the Michaelis–Menten formalism has led to alternative approaches involving linearlization around appropriate operating points (Hearon, 1953; Bak, 1963; Palsson & Lightfoot, 1984). The resulting linear formalism is among the best understood and developed mathematical structures. A linearized description of a biochemical system, therefore, can be efficiently treated mathematically in many different ways, even if there are hundreds of system components. It is a general symbolic formalism that is guaranteed to be valid at least over some restricted range of the concentration values. However, biochemical systems are often highly nonlinear and, for instance, can saturate or oscillate in stable cycles. As a result, the linear representation, which is valid only over a limited range of reactant and modifier concentrations around an operating point, cannot

adequately account for these more complex nonlinear behaviors.

The power-law formalism yields nonlinear representations of biochemical systems. It is based on a Taylor-series expansion in logarithmic space and only requires that the system constituents be positive and that the equations representing the processes within the biochemical system be differentiable. Biological systems represented by continuous vairables almost always satisfy these requirements. Although, from a mathematical standpoint, the power-law representation is an approximation, it has been demonstrated time and again that a host of biological phenomena actually show linear characteristics if plotted in logarithmic coordinates, which is equivalent to power-law characteristics in Cartesian coordinates. Power-law functions are found at various levels of organization in biochemical systems. Elemental chemical kinetics are based on the probability of association of molecules, which naturally leads to power-law functions [Vol'pert & Khudyaev, 1975; Chapter 2 of Savageau (1976)]. The relative change of one chemical substance with respect to another during growth and development often obeys a power-law function (Needham, 1950). Kohen et al. (1974) found that the kinetics of individual biochemical reactions within living cells are described by power-law functions of the reactant concentrations. Genetic regulation is often characterized by straight lines in logarithmic coordinates [Chapter 14 of Savageau (1976)]. Interactions between cells and biochemical mediators were represented by power-law functions and yield excellent agreement with experimental data (Voit & Savageau, 1982a).

In systematically elaborating the power-law formalism, one of the first features to be recognized was its "telescopic" property. One can describe the elemental processes on a fine scale, or one can aggregate them into net processes and describe them on a coarser scale, and each level continues to be described by power-law functions (Savageau, 1969a,b, 1985a). This property implies alternative strategies for representing a given phenomenon and raises the question of which modeling strategy is best. Alternative strategies were originally explored with mathematical tractability as the criterion for optimality. It was found that aggregation into two rate laws, one for the net increase and one for the net decrease of a given system constituent, was optimal; consequently, this variant of the power-law formalism was used as the basis for biochemical systems theory (Savageau, 1969a,b, 1970, 1971a,b). Important questions about steady states, dynamic solutions, stability, and system sensitivity to parameter variation can be answered readily in the power-law formalism by following the strategy of aggregation. In contrast, the evaluation of these system features poses serious mathematical difficulties if one does not aggregate into rate laws for net increase and net decrease but rather aggregates the mechanistic steps and represents each rate process by an individual power-law function. Examples of this strategy are the rate laws $V_{P-}$ considered above. On the other hand, one could aggregate even the rate laws for net increase and net decrease into just one power-law function, but the resulting representation then looses important features that are very common in biochemical systems.

The analytical disadvantages of these alternative power-law representations might be tolerated if these representations were significantly more accurate than that involving aggregation into two rate laws for net increase and net decrease of each system constituent. Thus, in this paper we have compared the alternative modeling strategies with accuracy of representation as the criterion. Because of their prominent role in biochemistry, we have used MMRL and HRL as references. Mathematically these rate laws are simple functions, but their sums exhibit locally all types of curvature and inflection. Hence, the methods that we developed to treat these features are general enough to cover the full spectrum of local behavior for other rate laws as well. Our topological methods can be applied directly to other continuous functions and will yield the same results; our quantitative measures, such as range of validity or superiority, also are general enough to characterize any rate law or continuous function, although the numerical results will depend on the parameter values. Thus, this methodology is not restricted to specific cases, such as MMRL and HRL, but applies to biochemical rate laws in general.

Our results show that the nonlinear power-law representations are usually more accurate than the linear representation. This superiority in accuracy is reflected in the range of validity within which the actual rate law and the power-law or the linear representation differ at most by a given amount. This range is in most relevant cases significantly wider if one chooses the power-law representation with aggregation into rate laws for net increase and net decrease rather than the power-law representation for each individual rate law or the linear representation. Another criterion for accuracy was defined in terms of random perturbations from a given set of operating values. All natural systems are exposed to such perturbations. Again, the power-law representation with aggregation into rate laws for net increase and net decrease was superior under most relevant conditions. These results might be surprising at first glance, because intuition could suggest that representing each reaction and then collecting all representations would yield the best description. However, the above results demonstrate that it is more accurate first to aggregate all reactions that increase and all those that decrease a system constituent and then, as the very last operation, to represent the aggregated rate laws by power-law functions. One reason for the superiority of this strategy may be that converting to the power-law representation at the last step permits cancellations of deviations from the actual rate law. In contrast, conversion to the power-law representation at the first step might yield appropriate models for individual reactions, but in the integrated system differences between the power-law representations and reality might accumulate, leaving no chance for cancellation of errors.

The superior representation of diverging and converging reactions in the power-law formalism with aggregation into rate laws for net increase and net decrease suggests that this representation of an integrated biochemical system would be more accurate than that in the power-law formalism with other levels of aggregation, although this general question has yet to be studied in detail. As a matter of fact, one can conceive of biochemical systems and particular conditions in which all components are represented more accurately in the formalism with aggregation into rate laws for net increase and net decrease, and at the same time, some aspects of the integrated system are more accurately described in the formalism with alternative levels of aggregation, due to compensation of errors. Such cases may not be biologically significant, but they provide another caution that intuition is not sufficient as a tool for relating the behavior of intact systems to their underlying determinants.

The earlier mathematical considerations described above and the differences in accuracy demonstrated in this paper have a direct bearing on the relative merits of two of the most common variants of the power-law formalism. The variant that uses aggregation into rate laws for net increase and net decrease is the basis of biochemical systems theory. The

concepts of this theory were established in the late sixties (Savageau, 1969a,b, 1970, 1971a,b, 1972), and due to its mathematical tractability, the repertoire of analyses and applications has steadily grown since then. On the other hand, the method of metabolic control, as subsequently proposed by Kacser and Burns (1973) and Heinrich and Rapoport (1974), is based on a special case of the power-law formalism with aggregation into individual rate laws for each reaction (Savageau et al., 1987a,b). Many concepts of metabolic control have followed earlier analogous developments in biochemical systems theory (Voit, 1987), whereas there are still no concepts or results in the framework of metabolic control that are not also present in biochemical systems theory. In contrast, biochemical systems theory contains a variety of methods and general results that cannot be obtained with the current version of metabolic control. Examples are steady-state and stability calculations, the dynamics of biochemical systems, and general analyses of biological design principles [e.g., see Savageau (1985a,b), Irvine and Savageau (1985a,b), and Savageau et al. (1987a,b)]. From the results in this paper we conclude that the variant of the power-law formalism that underlies biochemical systems theory is generally more accurate a representation of biochemical systems than the variant that underlies metabolic control.

We now return to the second general question stated in the introduction, Why the range of validity of power-law representations is so amazingly wide, in some cases 100–1000-fold [e.g., Chapters 13 and 14 of Savageau (1976)]. Although we do not fully understand why this exceptional accuracy occurs, we can now enumerate at least four contributing factors. (1) To some extent, this wide range is due to the mathematical nature of the power-law formalism: The Taylor-series approximation is performed in logarithmic space and thus yields a nonlinear representation that is accurate over a much wider range than the conventional linear approximation. However, this argument does not suffice to explain sizes as large as 100- or 1000-fold for the range of validity. (2) Another explanation is the multitude of homeostatic regulatory mechanisms, like feedback loops, that are found in every biological system. These mechanisms effectively maintain many concentration variables within narrow limits, which tends to promote the accuracy of any representation based upon a Taylor-series approximation (Savageau, 1976). (3) Such regulatory mechanisms also tend to simplify the analytical form of rate laws in the intact system, as opposed to the form that would be obtained in isolation [Chapter 5 in Savageau (1976)]. The simplification that is observed empirically in technological systems is often linear (Truxal, 1955), but in biochemical systems, the resulting simplifcation is that of a power law (Savageau, 1976). (4) To the above, which have been noted previously, we can now add that aggregation into rate laws for net increase and net decrease improves the accuracy of representation.

Finally, we wish to point out that the S-system equations, which result from aggregation into rate laws for net increase and net decrease, not only are convenient and accurate for the analysis of biochemical systems but also are mathematically very interesting in themselves. It has been shown that most, if not all, mathematical descriptions of biological interest can be recast *exactly* as S systems (Savageau, 1979, 1980, 1982; Savageau & Voit, 1982, 1987; Voit & Savageau, 1984–1986), which illustrates the power and generality of the power-law formalism from a different perspective.

ACKNOWLEDGMENTS

We thank Dr. D. H. Irvine for his many helpful suggestions and for his constructive criticism of the manuscript.

REFERENCES

Atkinson, D. E. (1966) *Annu. Rev. Biochem. 35*, 85–124.
Bak, T. A. (1963) *Contributions to the Theory of Chemical Kinetics*, Benjamin, New York.
Baker, T. J., & Crawford, I. P. (1966) *J. Biol. Chem. 241*, 5577–5584.
Brown, W. E. L., & Hill, A. V. (1923) *Proc. R. Soc. London, B 94*, 297–334.
Cedar, H., & Schwartz, J. H. (1969) *J. Biol. Chem. 244*, 4122–4127.
Cleland, W. W. (1967) *Annu. Rev. Biochem. 36*, 77–112.
Dopheide, T. A. A., Crewther, P., & Davidson, B. E. (1972) *J. Biol. Chem. 247*, 4447–4452.
Duggleby, R. G., Sneddon, M. K., & Morrison, J. F. (1978) *Biochemistry 17*, 1548–1554.
Hearon, J. Z. (1953) *Bull. Math. Biophys. 15*, 121–141.
Heinrich, R., & Rapoport, T. A. (1974) *Eur. J. Biochem. 42*, 89–95.
Henderson, E. J., Nagano, H., Zalkin, H., & Hwang, L. H. (1970) *J. Biol. Chem. 245*, 1416–1423.
Irvine, D. H., & Savageau, M. A. (1985a) *J. Immunol. 134*, 2100–2116.
Irvine, D. H., & Savageau, M. A. (1985b) *J. Immunol. 134*, 2117–2130.
Ito, J., & Yanofsky, C. (1969) *J. Bacteriol. 97*, 734–742.
Kacser, H., & Burns, J. A. (1973) *Symp. Soc. Exp. Biol. 27*, 65–104.
Koch, G. L. E., Shaw, D. C., & Gibson, F. (1971) *Biochim. Biophys. Acta 229*, 795–804.
Kohen, E., Thorell, B., Kohen, C., & Solmon, J. M. (1974) *Adv. Biol. Med. Phys. 15*, 271–297.
Koshland, D. E., Nemethy, G., & Filmer, D. (1966) *Biochemistry 5*, 365–385.
Michaelis, L., & Menten, M. L. (1913) *Biochem. Z. 49*, 333–369.
Monod, J., Wyman, J., & Changeux, J.-P. (1965) *J. Mol. Biol. 12*, 88–118.
Needham, J. (1950) *Biochemistry and Morphogenesis*, University Press, Cambridge, England.
Pabst, M. L., Kuhn, J. C., & Somerville, R. L. (1973) *J. Biol. Chem. 248*, 901–914.
Palsson, B. O., & Lightfoot, E. N. (1984) *J. Theor. Biol. 111*, 273–302.
Patte, J.-C., Le Bras, G., & Cohen, G. N. (1967) *Biochim. Biophys. Acta 136*, 245–257.
Savageau, M. A. (1969a) *J. Theor. Biol. 25*, 365–369.
Savageau, M. A. (1969b) *J. Theor. Biol. 25*, 370–379.
Savageau, M. A. (1970) *J. Theor. Biol. 26*, 215–226.
Savageau, M. A. (1971a) *Nature (London) 229*, 542–544.
Savageau, M. A. (1971b) *Arch. Biochem. Biophys. 145*, 612–621.
Savageau, M. A. (1972) *Curr. Top. Cell. Regul. 6*, 63–130.
Savageau, M. A. (1976) *Biochemical Systems Analysis: A Study of Function and Design in Molecular Biology*, Addision-Wesley, Reading, MA.
Savageau, M. A. (1979) *Proc. Natl. Acad. Sci. U.S.A. 76*, 5413–5417.
Savageau, M. A. (1980) *Math. Biosci. 48*, 267–278.
Savageau, M. A. (1982) *Biom. J. 24*, 323–330.
Savageau, M. A. (1985a) *Biomed. Biochim. Acta 44*, 839–844.
Savageau, M. A. (1985b) *Biomed. Biochim. Acta 44*, 875–880.

Savageau, M. A., & Voit, E. O. (1982) *J. Ferment. Technol. 60*, 221–228.
Savageau, M. A., & Voit, E. O. (1987) *Math. Biosci.* (in press).
Savageau, M. A., Voit, E. O., & Irvine, D. H. (1987a) *Math. Biosci. 86*, 127–145.
Savageau, M. A., Voit, E. O., & Irvine, D. H. (1987b) *Math. Biosci. 86*, 147–169.
Schmidt, J. C., & Zalkin, H. (1969) *Biochemistry 8*, 174–181.
Schmidt, J. C., & Zalkin, H. (1971) *J. Biol. Chem. 246*, 6002–6010.
Schmidt, J. C., Artz, S. W., & Zalkin, H. (1970) *J. Biol. Chem. 245*, 4019–4027.
Thomas, G. B., Jr., & Finney, R. L. (1982) *Calculus and Analytical Geometry*, 5th ed., Addison-Wesley, Reading, MA.
Truffa-Bachi, P., & Cohen, G. N. (1966) *Biochim. Biophys. Acta 113*, 531–541.
Truxal, J. G. (1955) *Automatic Feedback Control System Synthesis*, McGraw-Hill, New York.
Voit, E. O. (1987) *Trends Biochem. Sci. (Pers. Ed.) 12*, 221.
Voit, E. O., & Savageau, M. A. (1982a) *J. Ferment. Technol. 60*, 229–232.
Voit, E. O., & Savageau, M. A. (1982b) *J. Ferment. Technol. 60*, 233–241.
Voit, E. O., & Savageau, M. A. (1984) *J. Math. Anal. Appl. 103*, 380–386.
Voit, E. O., & Savageau, M. A. (1985) *Lect. Notes Biomath. 57*, 517–524.
Voit, E. O., & Savageau, M. A. (1986) *Math. Biosci. 78*, 47–55.
Vol'pert, A. I., & Khudyaev, S. I. (1975) *Analiz v Klassakh Razryvnych Funktsii i Uravneniya Matematicheskoi Fiziki*, p 351, Izdatel'stvo Nauka, Moskva.
Weitzman, P. D. J., & Wilson, I. B. (1966) *J. Biol. Chem. 241*, 5481–5488.
Welch, G. R., & Keleti, T. (1987) *Trends Biochem. Sci. (Pers. Ed.) 12*, 216–217.
Wong, J. T.-F., & Hanes, C. S. (1962) *Can. J. Biochem. Physiol. 40*, 763–804.

# Oxygenation of Trans Polyunsaturated Fatty Acids by Lipoxygenase Reveals Steric Features of the Catalytic Mechanism†

Max O. Funk, Jr.,* Jon C. Andre,‡ and Tetsuo Otsuki§
*Department of Chemistry, University of Toledo, Toledo, Ohio 43606*
*Received March 20, 1987; Revised Manuscript Received May 15, 1987*

ABSTRACT: Lipoxygenase, a nonheme iron dioxygenase, catalyzes the oxygenation of 1,4-diene units in polyunsaturated fatty acids, forming conjugated diene hydroperoxides as the primary products. The naturally occurring all-*Z* geometry for the olefins in the polyunsaturated fatty acid has long been thought to be a substrate requirement for the enzyme. A rigorous test of this hypothesis using the two isomeric (9*E*,12*Z*)- and (9*Z*,12*E*)-9,12-octadecadienoic acids was carried out. Both isomeric substrates were found to be catalytically oxygenated by soybean lipoxygenase 1 at a significant fraction of the rate of the reaction of the natural substrate, linoleic acid. Product determinations revealed that a thermodynamically unfavorable *E* to *Z* isomerization at the 9,10-position occurred when (9*E*,12*Z*)-9,12-octadecadienoic acid was converted into the 13-hydroperoxide by lipoxygenase 1. Determination of the stereochemistry at the oxygenated position in the products indicated that a comparable isomerization at the 12,13-position did not occur when the 9*Z*,12*E* isomer was employed. The distribution of products obtained from oxygenation at the 9-position supported the hypothesis that the enzyme catalyzes the reaction in one of two substrate orientations, conventional and head to tail reversed. The observations can be understood on the basis of the steric demands on intermediates in the proposed mechanism of action as well as by catalysis by the active-site iron atom.

The enzyme lipoxygenase is a nonheme iron dioxygenase that plays a major role in polyunsaturated fatty acid metabolism in both plants and animals. In plants, it has recently been demonstrated that lipoxygenase catalysis is part of a biosynthetic sequence leading to growth regulatory substances (Vick & Zimmerman, 1984). In animals, the enzyme catalyzes the inaugural step in the conversion of arachidonic acid into the leukotrienes, a family of compounds with various potent physiological activities (Samuelsson, 1983). The enzyme from soybeans has received the most attention in terms of a detailed physical and chemical characterization because of its early discovery (Theorell et al., 1947), abundance, ease of isolation, and stability (Finnazzi-Agro et al., 1973).

The oxygenation of polyunsaturated fatty acids catalyzed by lipoxygenase 1 from soybeans has long been thought to be specific for substrates containing the (*Z*,*Z*)-1,4-pentadiene structural unit at an appropriate location in the carbon chain (Holman et al., 1968). While the positional specificity of the enzyme for different polyunsaturated fatty acids and the composition of products obtained from these oxygenations have been extensively studied (Hamberg & Samuelsson, 1967), the

† This research was supported financially by the National Institutes of Health and the D'Arce Memorial Endowment for Biomedical Research. M.O.F. is the recipient of a Research Career Development Award from the National Institutes of Health.
* Address correspondence to this author.
‡ Present address: Department of Chemistry and Biochemistry, University of Maryland, College Park, MD 20742.
§ Present address: Department of Chemistry, Occidental College, Los Angeles, CA 90041.

0006-2960/87/0426-6880$01.50/0 